*Iranian Journal of Hydrogen & Fuel Cell 4(2016) 315-322*

Iranian Journal of Hydrogen & Fuel Cell

IJHFC

Journal homepage://ijhfc.irost.ir

# Investigation of the catalytic performance and coke formation of nanocrystalline Ni/SrO-$Al_2O_3$ catalyst in dry reforming of methane

**Elaheh Amir[1], Mehran Rezaei[1, 2*] , Fereshteh Meshkani[1]**

[1]Catalyst and Advanced Materials Research Laboratory, Chemical Engineering Department, Faculty of Engineering, University of Kashan, Kashan, Iran

[2]Institute of Nanoscience and Nanotechnology, University of Kashan, Kashan, Iran

**Article Information**

Article History:

Received:
16 Jan 2017
Received in revised form:
19 Apr 2017
Accepted:
06 May 2017

**Keywords**

Nickel catalyst
Strontium
Dry reforming
Nanocrystalline

**Abstract**

In this study, nickel catalysts supported on mesoporous nanocrystalline gamma alumina promoted by various strontium contents were prepared by the impregnation method and employed in dry reforming of methane (DRM). The prepared catalysts were characterized using $N_2$ adsorption (BET), temperature-programmed reduction and oxidation (TPR,) and oxidation (TPDTPO), X-ray diffraction (XRD), and scanning electron microscopy (SEM) techniques. TPR analysis revealed that the increases in Sr content enhanced the reducibility of the catalysts. The obtained results indicated that increasing Sr content increased both the methane and carbon dioxide conversions. In addition, the $CO_2$ conversion was higher than the $CH_4$ conversion due to the occurrence of the reverse water gas shift reaction. Among the studied catalysts, Ni/10% Sr-$Al_2O_3$ exhibited the highest catalytic activity and the lowest carbon formation. This catalyst showed high stability without any decrease in methane conversion up to 12 h of reaction. The results of this study could be employed in developing an industrial catalyst for the dry reforming reaction.

## 1. Introduction

Synthesis gas is composed of hydrogen and carbon monoxide which is employed in numerous metallurgical and chemical processes, it is also very important as a raw material in the petrochemical industry [1]. Catalytic reaction of carbon dioxide reforming of methane (Eq.1) is one of the methods to produce synthesis gas. This reaction with the consumption of two greenhouse gases, $CH_4$ and $CO_2$, has attracted much attention due to its economical and environmental aspects. Furthermore, dry reforming of methane is an effective method for the production of syngas with a lower $H_2$/CO ratio which is desirable

*Corresponding Author's Fax:+98 3155511121
E-mail address: rezaei@kashanu.ac.ir

for many of industrial reactions such as synthesis of oxygenated compounds and production of liquid hydrocarbons in the Fischer-Tropsch process [2-5].

$$CH_4+CO_2 \leftrightarrow H_2+CO \qquad \Delta H=247.3\ kJ/mol \qquad (1)$$

However, the major problem of dry reforming of methane is its high tendency for coke formation accumulating on the metal and the support of the catalyst. Nickel is used frequently in the study of dry reforming of methane due to its higher reactivity, availability and lower cost in comparison with noble metals [6-8]. Moreover, nickel catalysts are investigated extensively by $SiO_2$ and $Al_2O_3$ supports in DRM. The results show that the $Ni/Al_2O_3$ and $Ni/SiO_2$ catalysts exhibited high initial conversion. However, these catalysts also show high deactivation rates due to carbon deposition or sintering during the reaction. Several methods are utilized to enhance the resistance of these catalysts against carbon formation in the dry reforming process such as the addition of promoters, using different supports and preparation methods, etc. [9-12]. Alkaline promoters such as alkali and alkaline earth metals are able to change the nature of the support because of the high adsorption of carbon dioxide on the surface of the alkaline catalysts [8]. Large parts of the catalyst surface are masked in the low partial pressure of $CO_2$; consequently, this leads to coke deposition prevention on the surface of the catalyst [8]. In some reports, Sr is utilized as an alkaline earth promoter to improve the catalytic performance [13-16]. Strontium can catalyze the $CO_2$ gasification of the carbon formed during the reaction (reverse of reaction (2)).

$$2CO \leftrightarrow CO_2+C \qquad (2)$$

In this work, the effects of Sr addition on the physicochemical and catalytic properties of the nickel catalyst supported on alumina were investigated. In addition, the effect of Sr on the coke suppression of nickel catalysts in dry reforming was investigated.

## 2. Experimental

### 2.1. Catalysts preparation

In this study, Ni/xwt.%Sr-$Al_2O_3$ (x=0, 3, 5, 7, 10) catalysts were synthesized by a wet impregnation method. Nickel nitrate ($Ni(NO_3)_2.6H_2O$) and strontium nitrate ($Sr(NO_3)_2.4H_2O$) were used as Ni and Sr precursors, respectively. Also, boehmite (AlOOH) was used as the initial substance in the production of alumina as a catalyst support. To prepare these catalysts, the boehmite was first impregnated with an aqueous solution of strontium nitrate with an appropriate concentration for 4 h. After that, the impregnated powders were dried at 80 °C overnight and then calcined at 700 °C for 4 hours with a rate of 3°C/min. Then, the promoted support was impregnated with an aqueous solution of nickel nitrate according to the method described above. After impregnation, the catalysts were calcined at 500 °C for 4h.

### 2.2. Characterization

X-ray diffraction (XRD) analysis was performed using an X-ray diffractometer (PANalytical X'Pert-Pro) with a Cu-Kα monochromatized radiation source and a Ni filter in the range $2\theta=10–80^{o}$. The crystallite size was calculated by the Debye-Scherrer equation. The BET area of the samples was determined by nitrogen adsorption using an automated gas adsorption analyzer (Tristar3020, Micromeritics). Temperature programmed reduction (TPR) analysis was conducted in a Micrometrics chemisorb 2750 instrument. In the TPR measurement, 100 mg of catalyst was subjected to a heat treatment (10 ºC/min) in a gas flow (30ml/min) containing a mixture of $H_2$: Ar (10:90). Prior to the TPR experiment, the samples were heat treated under an inert atmosphere (Ar) at 250ºC for 1h. The $H_2$ uptake amount during the reduction was measured using a TCD. Temperature programmed oxidation (TPO) of the spent catalysts was carried out using a similar apparatus by introducing a gas flow (30 mL/min) containing a mixture of $O_2$: He (5:95) and the temperature was increased up to 800˚C at a heating

rate of 10˚C/min. SEM analysis was performed with VEGA TESCAN operated at 30 kV.

### 2.3. Catalytic evaluation

The catalytic characteristics were determined in a quartz tubular fixed-bed continuous-flow reactor (i.d. 7 mm, 80 cm length) under atmospheric pressure. The calcined catalyst was pressed, crushed and then sieved to prepare granules (200 mg) with the specific sizes (35-60 mesh). Prior to the reaction, the samples were reduced in a gas flow (20 mL·min$^{-1}$) at 600˚C for 4h. The reactant gas feed, consisting of $CH_4$ and $CO_2$, was introduced into the reactor (40 ml/min) and the activity tests were performed at different temperatures ranging from 550 to 700˚C in steps of 50˚C. The gas composition of reactants and products were analyzed using a gas chromatograph (Varian 3400) equipped with a TCD and a Carboxen 1000 column.

## 3. Results and discussion

### 3.1. Structural properties of the catalysts

The XRD patterns of the Ni catalysts and promoted catalysts with various percentages of strontium are displayed in Fig. 1. The diffraction peaks at 2θ= 37.4, 43.5, 63.1, 75.6° are assigned to the NiO phase (code N. 73-1519), and the observed peaks at 2θ= 37.4, 46.07, 66.9º are attributed to the alumina phase (code N. 01-1303).

The 5%Ni/$Al_2O_3$ catalyst showed three major crystallite phases: γ-$Al_2O_3$, NiO, and nickel aluminate ($NiAl_2O_4$). γ-$Al_2O_3$ has a pseudo spinel structure. The lattice parameters of gamma alumina are very close to that of $NiAl_2O_4$ [10]. This made the identification of these phases difficult due to peak overlapping. Fig. 1 also shows that peaks related to NiO were observed on the 5% Ni/$Al_2O_3$ catalyst, due to the low dispersion of NiO over the catalyst support. The diffraction peaks of NiO become more intense and sharper as Sr content decreases. As a result, the most intense peaks in the NiO phase belong to the

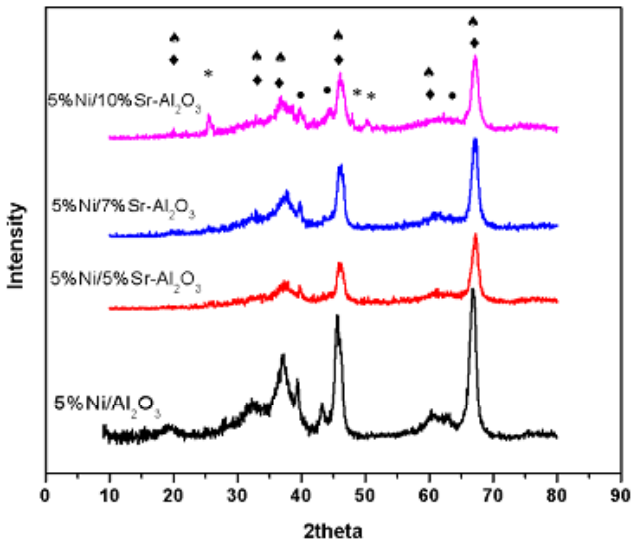


**Fig.1. XRD patterns of 5%Ni/Sr-$Al_2O_3$ catalysts with different percentages of Sr promoter. (♠: γ-$Al_2O_3$ ♦: $NiAl_2O_4$ ●: NiO *: $SrAl_2O_4$).**

5Ni/$Al_2O_3$ catalyst. The decrease in NiO peak intensities with the addition of Sr is related to a higher dispersion of nickel oxide over the promoted catalysts.

It can also can be seen that no peaks related to strontium phases were observed on the catalysts with a strontium content up to 10 wt.% due to the low content or high dispersion of strontium on the catalysts. It is seen that a peak corresponding to $SrAl_2O_4$ appears in catalysts with a 10 wt.% Sr, which reflects the composition of strontium oxide and alumina in high percentages of strontium.

The nitrogen adsorption-desorption isotherms and BJH pore size distribution for catalysts with different contents of strontium are displayed in Fig. 2. According to IUPAC classifications, all of the samples exhibit a type IV isotherm with a $H_3$ hysteresis loop related to the mesopore structure. The $H_3$ hysteresis is usually found on solids consisting of aggregates or agglomerates of particles forming slit-shaped pores (plates or edged particles like cubes) with nonuniform size and/or shape.

In addition, considering the similarity of the hysteresis loops it can be inferred that the shape of the pores is constant. Fig. 2b shows the pores size distribution of

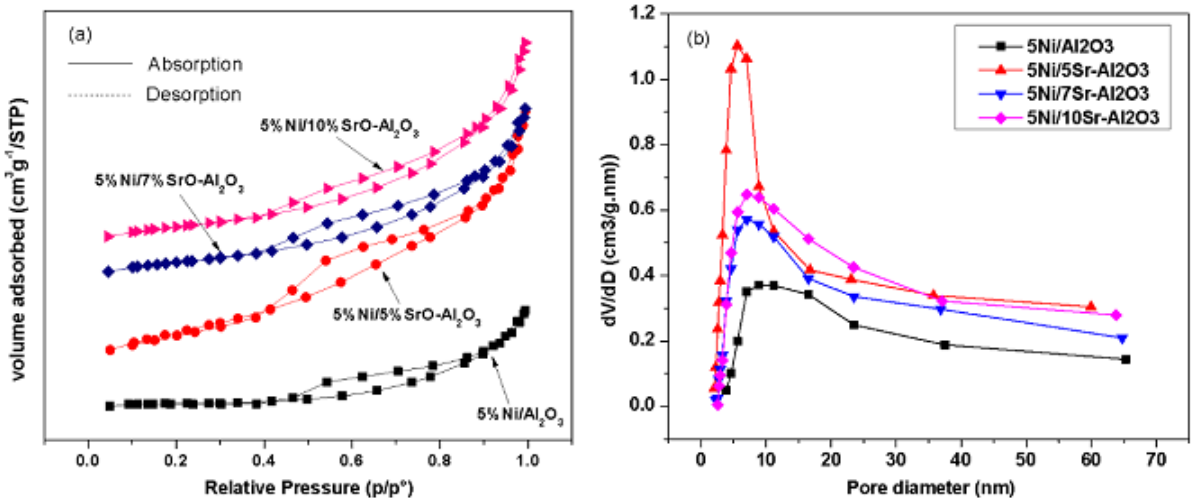


**Fig. 2. a) adsorption/desorption isotherms, b) pore size distribution.**

the catalysts. It is seen that the addition of promoter affected the pore size distribution. It seems that the addition of Sr shifted the maximum value of the pore size distribution curve to smaller sizes.

Table 1 represents the structural properties of the catalyst support and promoted support with different Sr contents. Increases in Sr content decreased the BET area and pore volume of the support. The reduction in BET area and pore volume was due to the partial blockage of the $Al_2O_3$ pores by strontium oxide clusters and/or a partial collapse of the mesoporous structure.

**Table 1. Structural properties of supports with various Sr contents**

| Support | Surface area ($m^2\ g^{-1}$) | Pore volume ($cm^3\ g^{-1}$) | Pore size (nm) |
|---|---|---|---|
| $\gamma$-$Al_2O_3$ | 37.7 | 0.08 | 6.6 |
| 5%Sr-$Al_2O_3$ | 36.7 | 0.07 | 7.7 |
| 7%Sr-$Al_2O_3$ | 30.1 | 0.06 | 8.1 |

The structural properties of the 5 wt.% nickel catalyst supported on alumina with different promoter contents are shown in Table 2. It is seen that the promoted catalysts possessed higher surface area and pore volume compared to the unprompted catalyst. As can be seen, there was no specific trend in surface area corresponding to increases in strontium content. It is seen that the Ni/5%Sr-$Al_2O_3$ catalyst exhibited the highest BET area due to the smallest pore size, Table 2.

**Table 2. Structural properties of catalysts with various Sr contents**

| catalyst | Surface area ($m^2\ g^{-1}$) | Pore volume ($cm^3\ g^{-1}$) | Pore size (nm) |
|---|---|---|---|
| 5%Ni/$Al_2O_3$ | 23.0 | 0.04 | 7.9 |
| 5%Ni/5%Sr-$Al_2O_3$ | 58.2 | 0.10 | 6.8 |
| 5%Ni/7%Sr-$Al_2O_3$ | 34.3 | 0.07 | 7.7 |
| 5%Ni/10%Sr-$Al_2O_3$ | 36.7 | 0.08 | 8.5 |

Fig. 3 illustrates the temperature-programmed reduction profiles of the Ni/$Al_2O_3$ catalysts with various Sr contents.

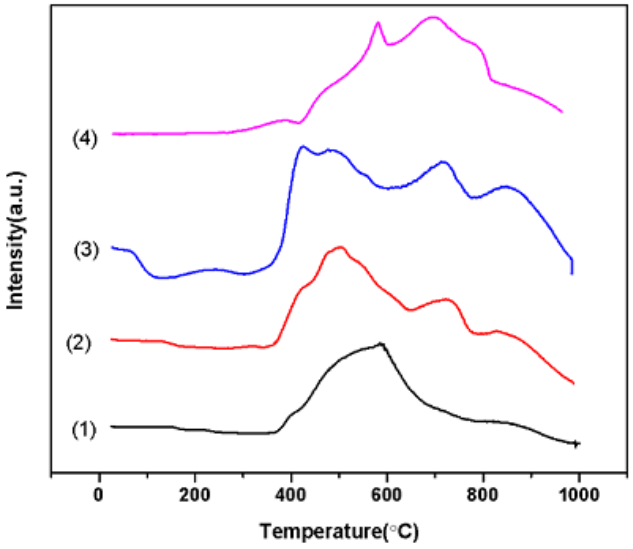


**Fig. 3. TPR profiles of Ni/x%Sr-$Al_2O_3$ catalysts with different Sr promoter loadings (1: x=0, 2: x=5, 3: x=7, 4: x=10**

TPR analysis indicates the different degree of interaction between the nickel species with catalyst support, which directly affects their reduction characteristics.

The TPR profile of the $Ni/Al_2O_3$ catalyst showed a strong interaction with the catalyst carrier with one major peak, $T_{max}$ at about 600˚C, which could be related to the reduction of NiO [18, 19]. With the addition of up to 7% promoter to the support , this reduction peak shifted to a lower temperature and slightly increased due to weaker metal-support interaction.

For the $Ni/Al_2O_3$ catalyst, two small shoulders peaks were observed at 400˚C and 850˚C. These peaks are attributed to the reduction of bulk nickel oxide and $NiAl_2O_4$, respectively [20-23]. The $NiAl_2O_4$ phase is primarily formed when Ni contacted strongly with $Al_2O_3$. This strong interaction improves the dispersion of Ni and might retard the sintering of Ni during the reforming process [25, 26]. Furthermore, it can be seen that the TPR profiles of $Ni/5\%Sr\text{-}Al_2O_3$ and $Ni/7\%Sr\text{-}Al_2O_3$ showed a reduction peak at 700˚C, which was ascribed to NiO species with a strong link with the catalyst support [27]. In the $Ni/10\%Sr\text{-}Al_2O_3$ catalyst, no reduction peaks were observed below 500˚C, associated with the bulk NiO phase. (unclear, did you mean, " In the $Ni/10\%Sr\text{-}Al_2O_3$ catalyst associated with the bulk NiO phase no reduction peaks were observed below 500˚C." or "In the bulk NiO phase, no reduction peaks were observed in the $Ni/10\%Sr\text{-}Al_2O_3$ catalyst below 500˚C."?) However, in the range of 500˚C to 800˚C high-intensity reduction peaks were observed. These results confirmed that the reducibility gradually improved with increases in Sr content up to 7%. But further increases in Sr content decreased the reducibility of a nickel catalyst. The raise and degradation of reduction temperature and the above mentioned affects can possibly be explained by the decoration effect of the strontium oxides with $Al_2O_3$ support and the metal Ni surface [28].

The results of catalytic activity at various reaction temperatures are shown in Fig. 4. As can be seen, both the $CH_4$ and $CO_2$ conversions improved with increases in reaction temperature due to the endothermic nature of the reaction. The increase in the percentage of the strontium improved both the methane and carbon dioxide conversions. According to Figs. 4a and 4b, the conversion of carbon dioxide is higher than the conversion of methane, which is due to the occurrence of the reverse water gas shift reaction.

The TPO analyses of the spent catalysts are shown in Fig. 5. All spent catalyst exhibited one peak at a temperature around 700°C, which is assigned to a filamentous form of carbon [4]. The accumulated carbon on the support could be combusted at a higher temperature than the carbon located on and near the active metal [28]. It is seen that the addition of strontium promoter to nickel catalyst decreased the

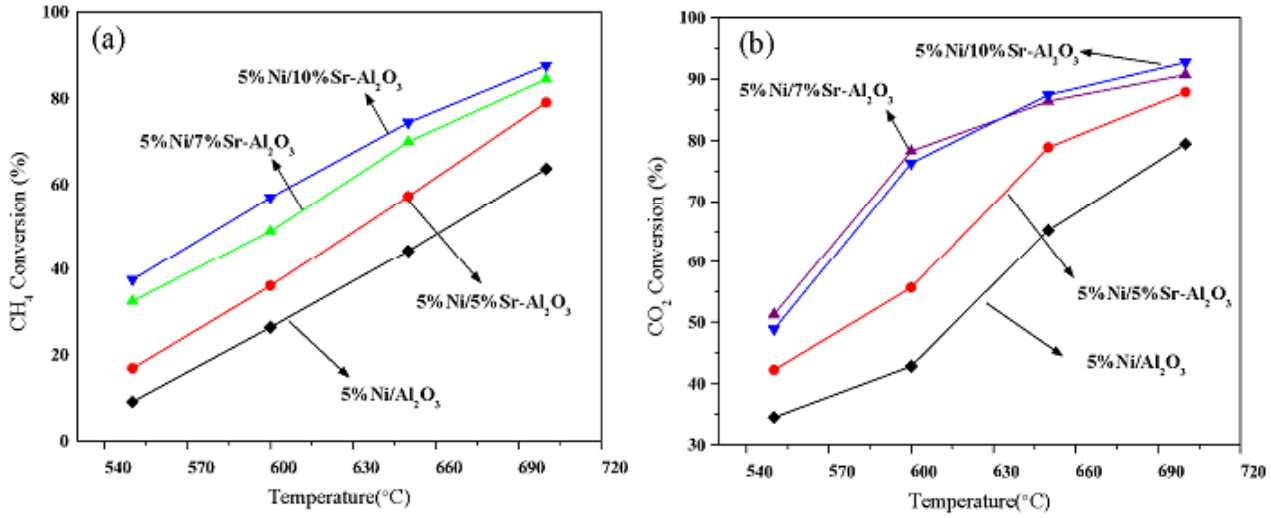


**Fig. 4. a) $CH_4$ conversion, b) $CO_2$ conversion. Reaction conditions: $CH_4/CO_2$ = 1/1, GHSV = 12,000(ml/h.$g_{cat}$)**

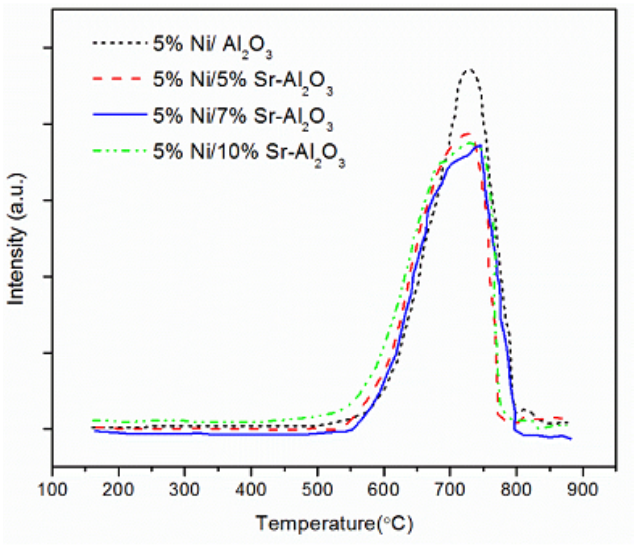


**Fig. 5. TPO profiles of spent catalysts with different loadings of Sr promoter (0%, 5%, 7% and 10%) after 15 h. Reaction condition: GHSV=12000(ml/g.h), $CH_4$:$CO_2$=1:1.**

amount of deposited carbon. In addition, by increasing Sr content from 5 to 10 wt.%, no considerable reduction in the area under the TPO curve was observed. The suppression of carbon formation on the promoted catalysts could be related to the higher dispersion of nickel on this catalyst due to a higher BET area. It is known that filamentous type carbon accumulation on the catalyst surface does not result in catalytic deactivation.

The SEM images of the spent $Ni/Al_2O_3$ and $Ni/Al_2O_3$ catalysts with 10% Sr promoter are shown in Figs. 6a and 6b, respectively. It is clear that filamentous type carbon was deposited over the spent catalysts. As can be seen, the filamentous carbon deposited on the $Ni/10\%Sr\text{-}Al_2O_3$ catalyst was less than that observed over the unpromoted catalyst. These results are in agreement with results obtained from the TPO analysis. However, filamentous type carbon did not decrease the catalytic activity. This type of carbon does not cover and block the active sites and pores and can only break down the catalyst particles and increase the reactor pressure drop.

The long-term stability of the $5\%Ni/10\%SrO\text{-}Al_2O_3$ catalyst is shown in Fig. 7. The result indicated that the $Ni/Al_2O_3$ catalyst with 10 wt.% Sr exhibited high stability during a 12 h time on stream.

## 4. Conclusions

In this article, the influences of the addition of strontium as a promoter on the physicochemical and catalytic characteristics of a $Ni/\gamma\text{-}Al_2O_3$ catalyst were investigated in a dry reforming reaction. The incorporation of strontium oxide enhanced the dispersion of NiO and the surface area of the catalysts. It was shown that the addition of strontium oxide up to 7 wt.% can improve the reducibility of $Ni/Al_2O_3$ catalyst. The catalytic results indicated that a raise in Sr content improved the methane and carbon dioxide conversions. It is seen that the addition of Sr to the catalyst reduced the formation

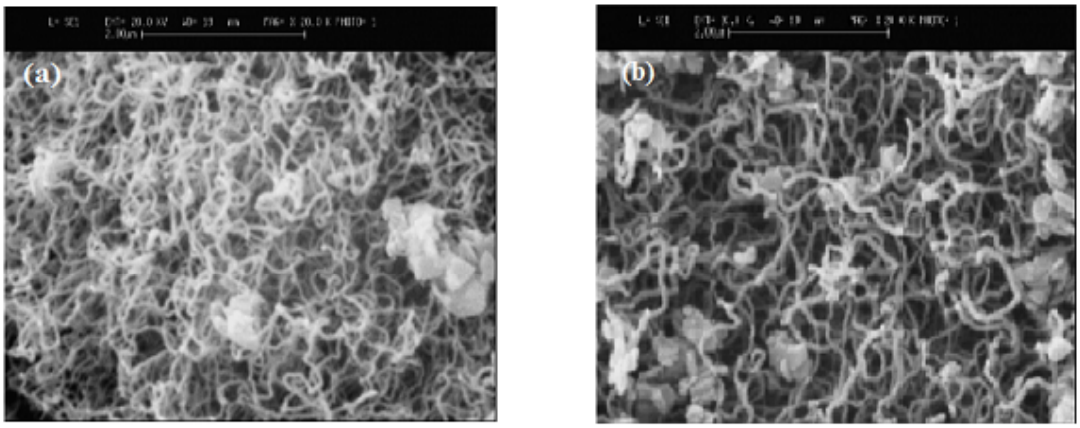


**Fig. 6. SEM images of spent a) $Ni/Al_2O_3$, b) $Ni/10\%Sr\text{-}Al_2O_3$ catalysts. Reaction condition: GHSV=12000(ml/g.h), $CH_4$:$CO_2$=1:1.**

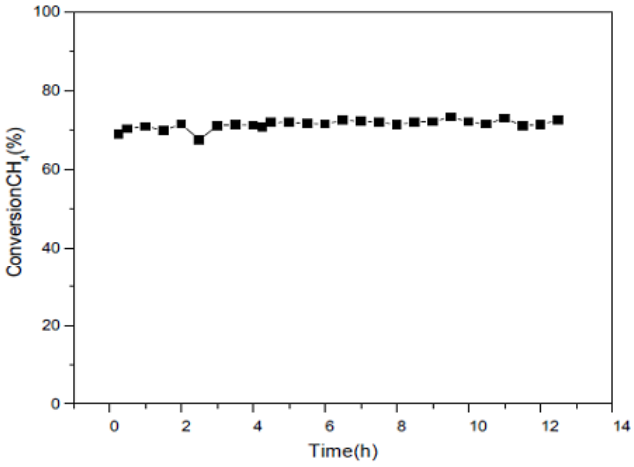


**Fig. 7. long time stability of 5%Ni/10%SrO-$Al_2O_3$ catalyst. Reaction condition: GHSV=12000(ml/g.h), $CH_4$:$CO_2$=1:1, T=650°C.**

of filamentous type carbon, which was confirmed by TPO and SEM analyses. The 5% Ni/10%Sr-$Al_2O_3$ catalyst exhibited very high stability during a 12 h time on stream. This sample can be considered as a promising catalyst for the production of synthesis gas from the catalytic dry reforming of methane.

## Acknowledgment

The authors are grateful to the University of Kashan for supporting this work by Grant No. 158426/42.

## References

[1] Goff. S. P., Wang S. I., "Syngas Production by Reforming", J. Chem. Eng. Prog., 1987, 83: 8.

[2] Jeong H., Kim K. I., Kim D., Song I. K., "Effect of promoters in the methane reforming with carbon dioxide to synthesis gas over Ni/HY catalysts", J. Molecular Catalysis A: Chemical, 2006, 246: 43.

[3] Nematollahi B., Rezaei M., Khajenoori M., "Combined dry reforming and partial oxidation of methane to synthesis gas on noble metal catalysts". int. J. hydrogen energy, 2011,28: 2969.

[4] Potdar H.S., Roh H.S., Jun K.W., Ji M., Liu Z.W. "Carbon dioxide reforming of methane over co-precipitated Ni-Ce-$ZrO_2$ catalysts. Catalysis letters", 2002, 84: 95.

[5] Meshkani F., Rezaei M., "Nanocrystalline MgO supported nickel-based bimetallic catalysts for carbon dioxide reforming of methane", int. J. hydrogen energy, 2010, 35: 10295.

[6] Alves H.J., Junior C.B., Niklevicz R.R., Frigo E.P., Frigo M.S., Coimbra-Araujo C.H., "Overview of hydrogen production technologies from biogas and the applications in fuel cells", int. J. hydrogen energy, 2013, 38: 5215.

[7] Wang S., Lu G.Q., Millar G.J., "Carbon dioxide reforming of methane to produce synthesis gas over metal-supported catalysts: state of the art", Energy & Fuels, 1996, 10: 896.

[8] Alipour Z., Rezaei M., Meshkani F., "Effect of alkaline earth promoters (MgO, CaO, and BaO) on the activity and coke formation of Ni catalysts supported on nanocrystalline $Al_2O_3$ in dry reforming of methane", J. Industrial and Engineering Chemistry, 2014, 20: 2858.

[9] Shekhawat II D., Spivey J. J., Berry D. A. editors, Fuel cells: technologies for fuel processing, Elsevier, 2011.

[10] Alipour Z., Rezaei M., Meshkani F., " Effect of K2O on the catalytic performance of Ni catalysts supported on nanocrystalline $Al_2O_3$ in $CO_2$ reforming of methane", Irainian journal of hydrogen & fuel cell, 2015, 2: 215-226.

[11] Zhang J., Ph.D. Thesis, University of Saskatchewan, 2009.

[12] Sutthiumporn K. and Kawi S., "Promotional effect of alkaline earth over Ni–$La_2O_3$ catalyst for $CO_2$ reforming of $CH_4$: role of surface oxygen species on $H_2$ production and carbon suppression" Int. J. Hydrogen Energy, 2011, 36: 14435.

[13] San José-Alonso D., Illán-Gómez M.J., Román-Martínez M.C., " K and Sr promoted Co alumina

supported catalysts for the $CO_2$ reforming of methane", Catalysis Today , 2011, 176 : 187–190.

[14] Jing Q., Lou H., Fei J., Hou Z., Zheng X., "Syngas production from reforming of methane with $CO_2$ and $O_2$ over Ni/SrO–$SiO_2$ catalysts in a fluidized bed reactor", Int. J. hydrogen energy, 2004, 29: 1245.

[15] Leofanti G., Padovan M., Tozzola G., Venturelli B., "Surface area and pore texture of catalysts", J. Catalysis Today, 1998, 41: 207.

[16] Cai X., Dong X., Lin W., "Effect of $CeO_2$ on the catalytic performance of Ni/$Al_2O_3$ for autothermal reforming of methane", J. Natural Gas Chemistry, 2008, 17: 98.

[17] Valentina R., Ph.D. Thesis, J. Alma Mater Digital-Università di Bologna 2007.

[18] Meshkani F., Rezaei M., Andache M., "Investigation of the catalytic performance of Ni/MgO catalysts in partial oxidation, dry reforming and combined reforming of methane", J. Industrial and Engineering Chemistry, 2014, 20: 1251.

[19] Kang K.M., Kim H.W., Shim I.W., Kwak H.Y., 2011, "Catalytic test of supported Ni catalysts with core/shell structure for dry reforming of methane", J. Fuel Processing Technology, 92: 1236.

[20] Ranjbar A., Rezaei M., "Preparation of nickel catalysts supported on CaO.2$Al_2O_3$ for methane reforming with carbon dioxide", int. J. hydrogen energy, 2012, 37: 6356.

[21] Joo O.S., Jung K.D., Han S.H., "Modification of H-ZSM-5 and gamma-alumina with formaldehyde and its application to the synthesis of dimethyl ether from syngas", J. Bulletin-Korean Chemical Society, 2002, 23: 1103.

[22] Cesteros Y., Fernandez R., Estellé J., Salagre P., Medina F., Sueiras J.E., Fierro J.L.G., "Characterization and catalytic properties of several LaNi and SrNi solids", J. Applied Catalysis A: General, 1997, 152: 249.

[23] Fei J., Hou Z., Zheng X. and Yashima T., "Doped Ni catalysts for methane reforming with $CO_2$", J. Catalysis letters, 2004, 98: 241.

[24] Lertwittayanon K., Atong D., Aungkavattana P., Wasanapiarnpong T., Wada S., Sricharoenchaikul V., "Effect of CaO–$ZrO_2$ addition to Ni supported on γ-$Al_2O_3$ by sequential impregnation in steam methane reforming" int. J. hydrogen energy, 2010, 35: 12277.

[25] Hou Z., Yokota O., Tanaka T., Yashima T., "Investigation of $CH_4$ reforming with $CO_2$ on meso-porous $Al_2O_3$-supported Ni catalyst", J. Catalysis Letters, 2003, 89: 121.